

Computational Study of Transverse Slot Injection in Supersonic Flow

Malsur Dharavath, P. Manna, and Debasis Chakraborty*

DRDO-Defence Research and Development Laboratory, Hyderabad - 500 058, India

*E-mail: debasis_cfd@drdl.drdo.in

ABSTRACT

The knowledge of transverse sonic injection flow field is very important for the design of scramjet combustor. Three dimensional Reynolds-Averaged Navier Stokes equations alongwith turbulence models are solved to find the effect of transverse sonic slot injection into a supersonic flow. Grid sensitivity of the results is studied for various structured grids. Simulations with different turbulence models (i.e., k- ϵ , k- ω , SST-k ω , and RNG-k ϵ) reveals that RNG-k ϵ turbulence model better predicts the flow features. Computational fluid dynamics predicted wall pressure distribution for various injection pressures matches well with experimental data. The extent of upstream separated region increases with the increase of the injection pressure. The increase of slot width makes the interaction between transverse jet and free stream more intense and causes more spreading and penetration of injectant in the downstream region.

Keywords: Supersonic flow; Transverse slot injection; Separation distance

1. INTRODUCTION

Due to very good mixing characteristics in supersonic flow, transverse slot injection has been studied extensively in hypersonic propulsion systems^{1,2}. Transverse slot injection is also used as thrust vector control (TVC) in rocket motors and hot/cold gas reaction system for missile control^{3,4}. The schematic of transverse slot jet interaction flow field is shown in Fig. 1. When a transverse flow comes through a slotted nozzle into supersonic flows, it expands and the blockage of free stream by secondary flow caused the formation of a strong bow shock, Mach disk and barrel shock in front of the injection point and the boundary layer separate. Just after the injection point, the boundary layer reattaches and a recompression shock wave is generated. The presence of boundary layer separation and Mach disk makes the flow very complex in both upstream and downstream of the injection point. Upstream separation length, Mach disk height, jet-to-cross flow momentum flux ratio, etc. characterise the transverse slot injection flow field in supersonic flows. The information of three-dimensional transverse injection flow field is very important for study of the mixing behaviour and evaluation of different aerospace systems performances.

Spaid and co-workers^{5,6} studied experimentally the influence of Mach number, pressure ratio and injectant gas composition for two-dimensional supersonic slot injection and found insensitiveness of upstream interaction to variations in the free stream Mach number and Reynolds number. The following general penetration formula of gaseous jets into supersonic flows was proposed by Portz & Segal⁷.

$$\frac{P}{D} = A \left(\frac{q_j}{q_\infty} \right)^B \left(\frac{x}{D} + C \right)^E \left(\frac{\delta}{D} \right)^F \left(\frac{W_j}{W_\infty} \right)^G \quad (1)$$

where P , D , δ , q , x and W represent jet penetration, jet diameter, boundary-layer thickness, dynamic pressure, downstream distance from injector centre and molecular weight, respectively, and the subscripts j and ∞ represent jet and free stream conditions.

The coefficients A , B , C , E , F , G are obtained from experimental measurements and are tabulated for different air stream Mach number⁷. Aso⁸, *et al.* conducted experimental studies of transverse gaseous nitrogen jet injection into external flow at Mach number of 3.8, total pressure of 1.2 MPa and Reynolds number of 2.0×10^7 through a transverse slot nozzle mounted on the flat plate. Separation region upstream of injection, the extent of the interaction region and shock structures increase with increase of total pressure and slot width.

Transverse sonic jet injections from flat plate into supersonic cross flow is numerically simulated extensively in recent literature. Both two dimensional⁹⁻¹² and three

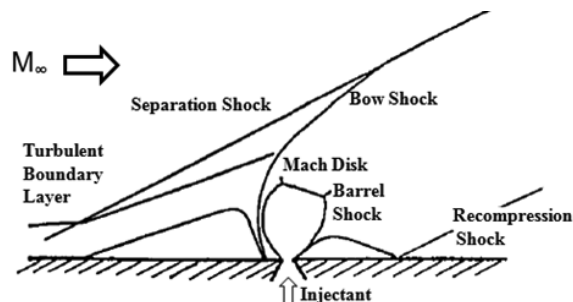


Figure 1. Schematic of transverse injection flow field.

dimensional¹³⁻¹⁸ RANS simulations, DES¹⁹ LES^{20,21} were reported. Rizetta¹⁰ performed two dimensional numerical simulation of Aso⁸, *et al.* experimental condition and compared the performance of $k-\epsilon$ and $k-\omega$ turbulence models in predicting various parameters. Complex turbulence structure with different length scales in the near-wall regions and in jet's counter rotating vortices exists in transverse jet and two dimensional simulations are highly inadequate to capture all the physical features.

Lee & Mitani¹⁵ studied the comparative performance of mixing augmentation in scramjet combustor for three transverse injectors by solving three dimensional RANS equations along with $k-\omega$ shear stress transport (SST) model. It is observed that jet to cross flow momentum ratio strongly effects the mixing characteristics. Higher values of momentum ratio causes slower mixing rates, higher penetration and more losses of stagnation pressure. Detailed structures of the Mach disc for transverse sonic injection in supersonic flow was captured by Sriram & Mathews¹⁶ through 3D RANS simulation with $k-\omega$ turbulence model. Computed results matched very well with experimental results in the upstream regions and close to the jet; while they differ by small amount in the downstream region. Huang¹⁸, *et al.* have performed 3D RANS simulation of the experimental work of Spaid & Zukowski⁵ using a commercial CFD solver and studied the effect of different turbulence models in predicting various features of the flow field. Different turbulence models predict different characteristics of upstream separation and height of Mach disc. It was observed that RNG- $k-\epsilon$ turbulence model performs better to predict the flow parameters. Although, recent DES¹⁹ LES^{20,21} studies provided better insights of complex mixing process of the problem, the application of these methods for engineering problems are still not very matured. It is clear that transverse injection into the supersonic stream is not fully understood and roles of various turbulence models in predicting this complex flow require further investigations. In the present work, three dimensional numerical simulation is performed for the experimental work of Aso⁸, *et al.* using a commercial CFD solver CFX²² 14.5 and the computed flow variables for different injectant and free stream pressure ratios are compared with the experimental results. Effects of different turbulence models and slot width are also studied parametrically.

2. EXPERIMENTAL WORK

The schematic of of Aso⁸, *et al.* experimental model is shown in Fig. 2. Gaseous Nitrogen from sonic throat is injected from a 1 mm width and 100 mm breadth slot into supersonic turbulent air stream. The model is mounted horizontally into the supersonic wind tunnel of cross section 150 mm x 150 mm. The slot nozzle is placed at 330 mm downstream from the leading edge of the flat plate. The experiments were conducted for free stream Mach number of 3.75-3.81, total pressure (P_0) of 1.20 Mpa and total temperature (T_0) of 283-299 K. Reynolds number (based on the distance between the flat plate leading edge and slot nozzle centre) was $1.03 \times 10^7 - 2.07 \times 10^7$. In the experiments, P_0 is kept constant whereas, $P_{0_{inj}}$ (total pressure of injected secondary flow) is changed from 0.1 MPa to 0.6 MPa to get different pressure ratios. The flow fields were

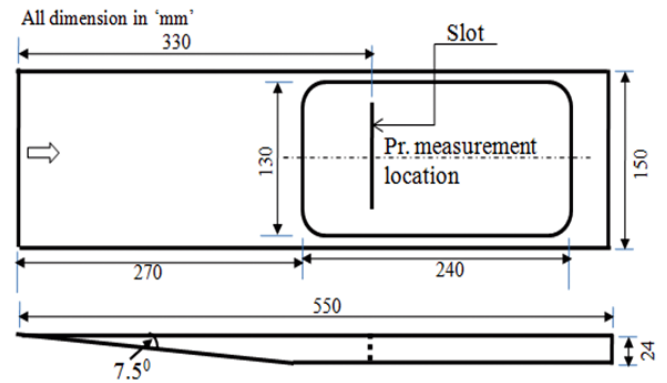


Figure 2. Flat plate models with slot nozzle.

visualised by the schlieren photography and static pressures were measured using multi-tube manometers.

3. COMPUTATION METHODOLOGY

ANSYS²² CFX-14.5, used in the present study, is an implicit finite volume method and is based on finite element approach to represent the geometry. The method retains much of the geometric flexibility of finite element methods as well as the important conservation properties of the finite volume method. The code solves 3D RANS equations with second order upwind discretisation of the convective term. Baseline calculations are done with $k-\epsilon$ turbulence model with wall function. Four different two-equation turbulence models, namely, $k-\epsilon$, $k-\omega$ and SST, RNG $k-\epsilon$ turbulence model are assessed for their predictive capabilities for mixing phenomena in supersonic flows with slot injection.

4. RESULTS AND DISCUSSIONS

4.1 Computational Domain, Grid Generation and Boundary Conditions

The flat plate geometry and the computational domain are shown in Fig. 3. The X , Y , and Z co-ordinate axes are taken along the longitudinal, transverse and lateral directions, respectively with the origin at the centreline of the slot nozzle. The computational domain is 600 mm, 250 mm, and 150 mm in the longitudinal, height and lateral directions respectively. The domain in longitudinal direction is extended 50 mm ahead of flat plate leading edge. Structured grid of 2.3 million cells size

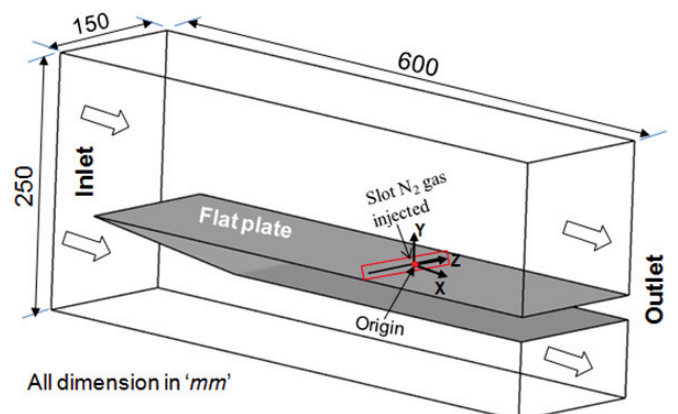


Figure 3. Computational domain with boundary details.

is employed in the computational domain. To capture the initial growth of the jet, fine meshes are employed near the inflow and the injected region. The grids are made progressively coarser in the downstream and far field regions. Stagnation pressure (1.20 MPa), temperature (299 K) and Mach number (3.75) are specified at the inlet boundary. Static pressure and supersonic boundary conditions are prescribed for the far field and outflow boundaries, respectively. No slip boundary and adiabatic wall conditions are imposed on the flat plate wall. Sonic Nitrogen gas is injected through slot injector at static temperature (T_{inj}) of 250 K. Jet-to-free stream pressure ratio (P_{inj}/P_{∞}) of 4.86, 10.29, 17.72, 25.15, 33.64, and 43.15 are considered in the simulation. A four order reduction of log-normalised maximum residue of various flow variables are considered for convergence criteria. Less than 1 per cent imbalance in global mass, momentum, and energy between outlet and inlet of the computational domain is achieved in the simulation.

4.2 Grid Independence Study

In present work, the grid independence study is performed with three different grid sizes, i.e., coarse grid 2.3 million ($295 \times 60 \times 130$), medium grid 2.9 million ($295 \times 70 \times 140$) and fine grid 3.49 million ($295 \times 79 \times 150$) cells for $P_{inj}/P_{\infty} = 25.15$ with standard $k-\epsilon$ turbulence model. The axial distributions of computed surface pressures with three different grids are as shown in Fig. 4. The pressures with medium and fine grids are almost identical demonstrating the grid independence of the results.

4.3 Effect of Turbulence Models on Wall Pressure

Four turbulence models namely, $k-\epsilon$, $k-\omega$, SST- $k\omega$ and RNG- $k\epsilon$ are assessed for their predictive capability of transverse gaseous injection from slot into the supersonic air stream. Fig. 5 shows the comparison of wall pressure profiles for 1 mm slot width with different turbulence models for $P_{inj}/P_{\infty} = 25.15$. RNG- $k\epsilon$ turbulence model shows better agreement with the experimental data including the length of upstream separation region compared to other three models. In the downstream of the injection, the results of all turbulence models match well with experimental results. The axial distribution of penetration and spreading of the injectant obtained from different turbulence models are compared for jet-to-free stream pressure ratio of 25.15 in Figs. 6(a) and 6(b). Penetration and spreading are defined as the injectant diffusion along the transverse and

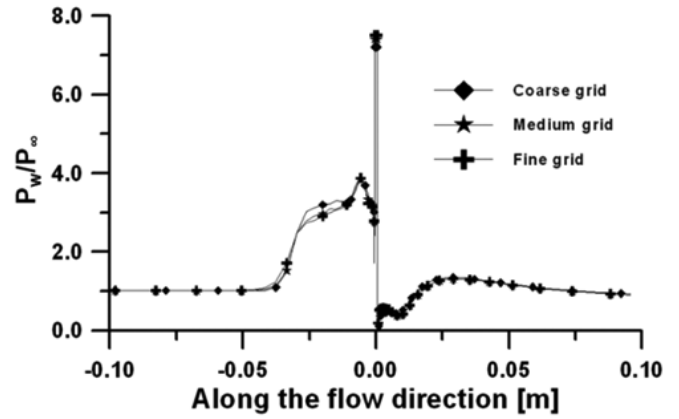


Figure 4. Comparison of wall pressure for different grids for $P_{inj}/P_{\infty} = 25.15$ at $Z = 0$.

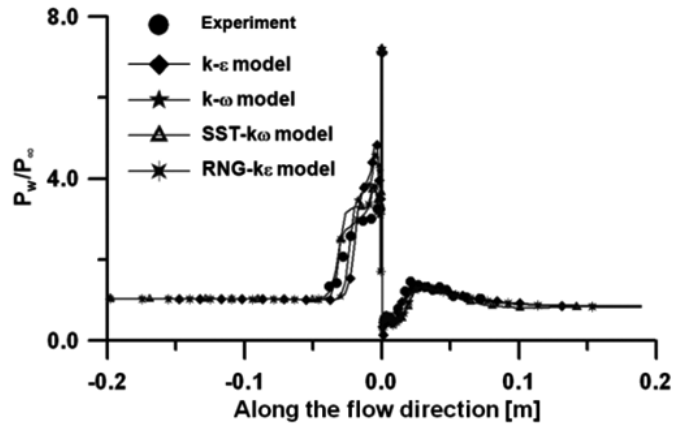


Figure 5. Comparison of wall pressure distributions with experiment data for $P_{inj}/P_{\infty} = 25.15$.

lateral direction respectively and they are normalised with the slot width (D). The penetration height and spreading distance of the injectant is found to be the highest for RNG $k-\epsilon$ turbulence model. The penetration height obtained with the empirical correlation (1) is also plotted in the Fig. 6(a). The coefficients of the empirical equation considered for the present case are as follows; $A = 4.2$, $B = 0.3$, $C = 0.0$, $E = 0.143$, $F = 0.057$, $G=0$, and Mach number of 4. The maximum difference of penetration between the RNG $k\epsilon$ turbulence model and the empirical correlation is as high as 100 per cent.

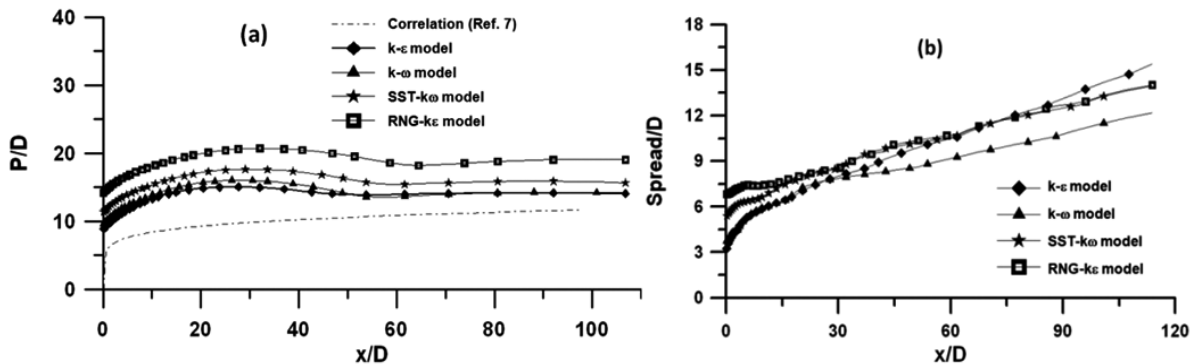


Figure 6. Comparison of axial distribution of (a) penetration and (b) spreading of the injectant for $P_{inj}/P_{\infty} = 25.15$ with different turbulence models.

4.4 Flow Field Analysis for $P_{inj}/P_\infty = 25.15$

The qualitative features of the transverse slot injection into supersonic flow for $P_{inj}/P_\infty = 25.15$ case are depicted through numerical schlieren in Fig 7. The simulation captures all the essential flow features like oblique shock at the leading edge of flat plate, bow shocks, barrel shocks, Mach discs and flow separation upstream of the injection points. Injected nitrogen gas interacts with the free-stream air flow and produces a strong bow shock. The interaction of bow shock with flat plate turbulent boundary layer causes boundary layer separation upstream of the slot. The recompression shock wave downstream of the slot is also observed. The blown up picture in Fig. 8 shows the Mach number distribution and streamline pattern of the flow in the injector region. The blockage of the free-stream flow by the injectant caused re-circulation zones both upstream and downstream of slot injector. The Mach disc and the barrel shock are clearly seen in the picture.

4.5 Effect of Slot Injector Pressure

Simulations were carried out for six different jet-to free stream pressure ratios ($P_{inj}/P_\infty = 4.86, 10.29, 17.72, 25.15, 33.65,$ and 43.15). Because of better predictive capability of RNG-k- ϵ model compared to other turbulence models in its class, we use RNG-k- ϵ model for further simulations. As was done in the experiment, free stream total pressure is kept fixed at 1.2 MPa and the secondary injection pressure was varied to obtain different pressure ratios. The axial distribution of static pressure in the flat plate and total pressure loss ($P_{0,loss}$) distribution for different pressure ratios are presented in Fig. 9. The total pressure loss is defined as:

$$P_{0,loss} = \left(1 - \frac{P_{0,x}}{P_0}\right) \times 100$$

where $P_{0,x}$ and P_0 are total pressure at local x location and free-stream total pressure, respectively.

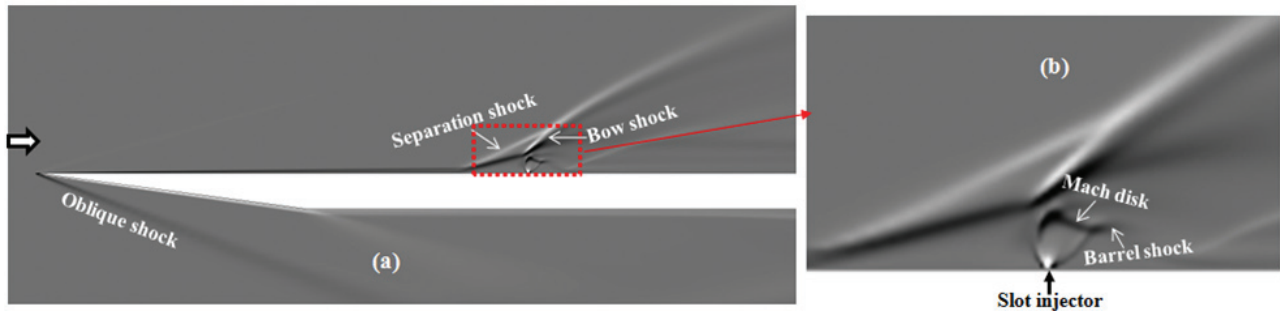


Figure 7. Computed density gradient for $P_{inj}/P_\infty = 25.15$ at mid width ($Z=0$ m) : (a) Shock structure on the flat plate and (b) Zoomed view near the slot injector.

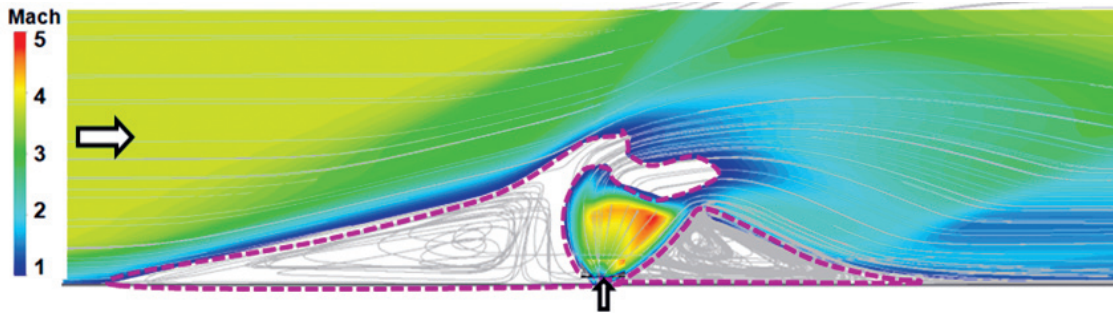


Figure 8. Composite picture of Mach number and streamline pattern near injector regions.

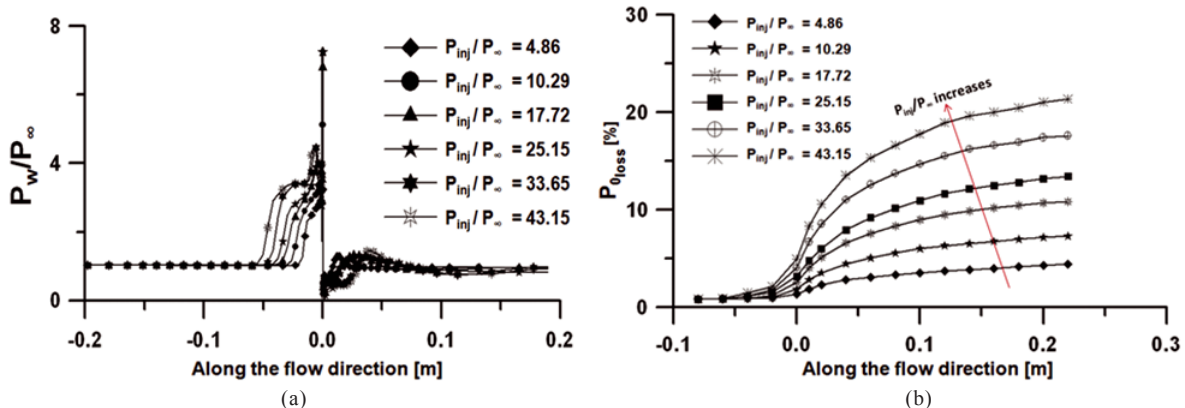


Figure 9. Axial distribution of (a) wall pressure and (b) total pressure loss with different jet to free stream pressure ratios.

As pressure ratio (P_{inj}/P_∞) increases, the interaction between the secondary flow and free stream pressure increases and the upstream separation point starts moving upstream. The upstream separation distance (X_{upsep}) and penetration height (h_{pen}) for different pressure ratios are shown in Fig. 10. The distance between the centre-line of the slot injector and the onset of separation is defined as separation distance. The height of the Mach disc from the flat plate wall is defined as penetration height. Both predicted upstream separation distance and penetration height increase with increase in the pressure ratios and match well with experimental data. Computed wall pressure distributions at mid-width ($Z = 0$) of flat plate for $P_{inj}/P_\infty = 4.86, 10.29, 17.72,$ and 25.15 are compared with experimental data in Figs 11(a) to 11(d), respectively and a reasonable good match between the two is obtained.

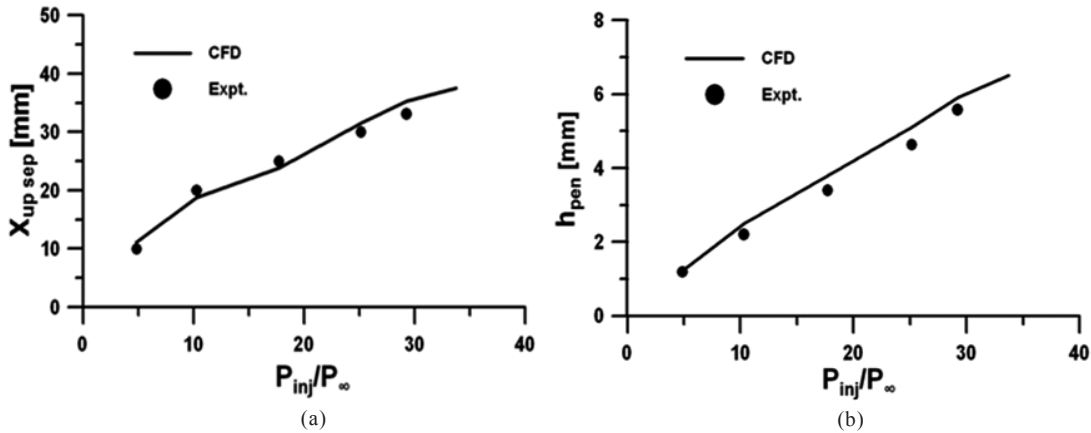


Figure 10. Comparison of (a) upstream separation distance and (b) penetration height with experimental data for different pressure ratios.

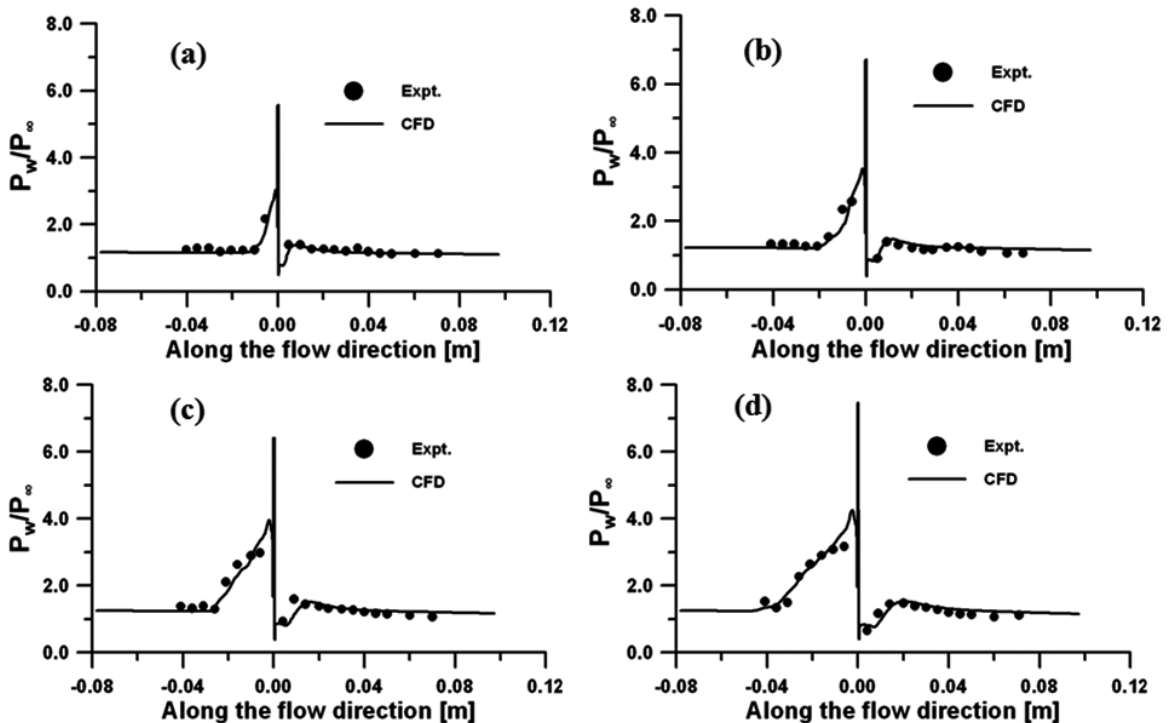


Figure 11. Wall pressure comparison with experimental data for different injection pressure: (a) $P_{inj}/P_\infty = 4.86$, (b) $P_{inj}/P_\infty = 10.29$, (c) $P_{inj}/P_\infty = 17.72$, and (d) $P_{inj}/P_\infty = 25.15$.

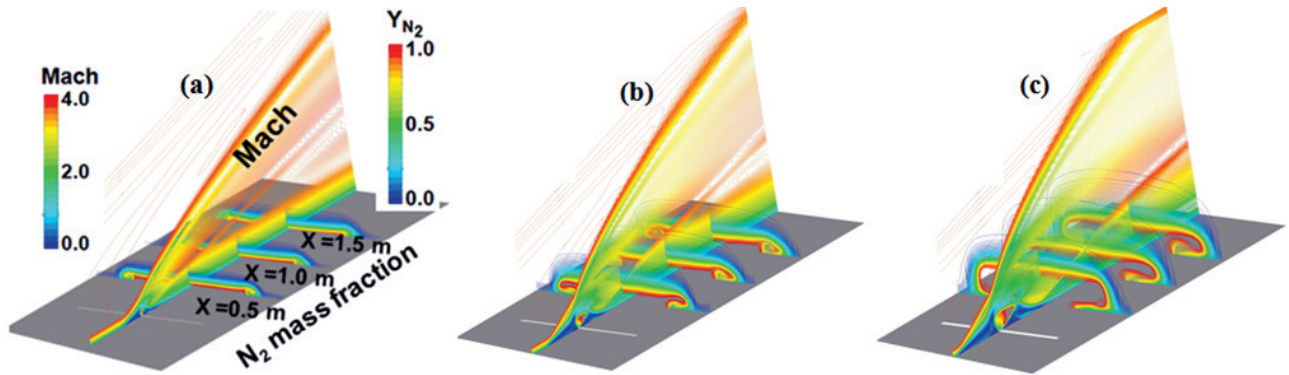


Figure 12. Composite picture of Mach number and injectant mass fraction for different slot width (a) 0.5 mm, (b) 1.5 mm, and (c) 3.0 mm.

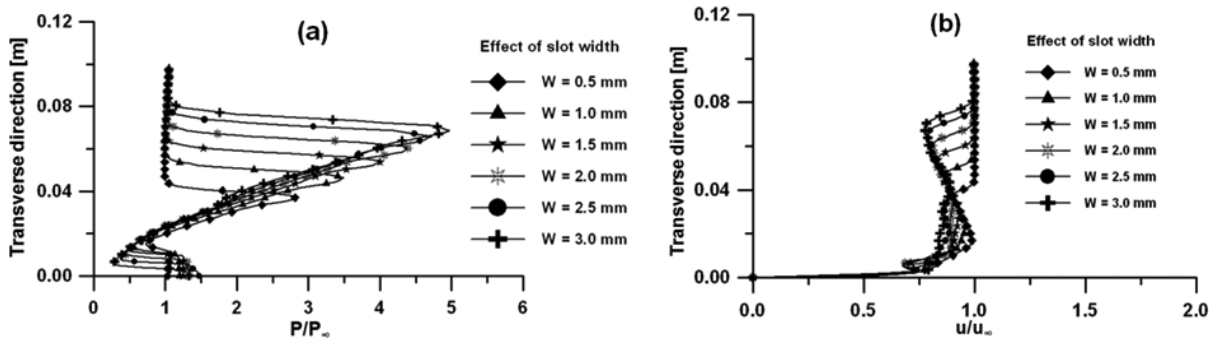


Figure 13. (a) Pressure and (b) velocity profiles at 50 mm downstream of the injector.

presented in Fig. 13. With the increase in the slot width, both pressure and velocity profiles are becoming much broader and intense. The maximum upstream separation distance and penetration height for different slot widths are presented in Fig. 14. More intense interaction between free stream and secondary flow due to increase in slot width is causing increase of both penetration height and upstream separation length. The maximum spread and penetration height for different pressure ratios for two different slot widths are compared in Fig. 15. Increase in slot widths is having more pronounced effect in spread compared to penetration for different jet – to – free stream pressure ratios.

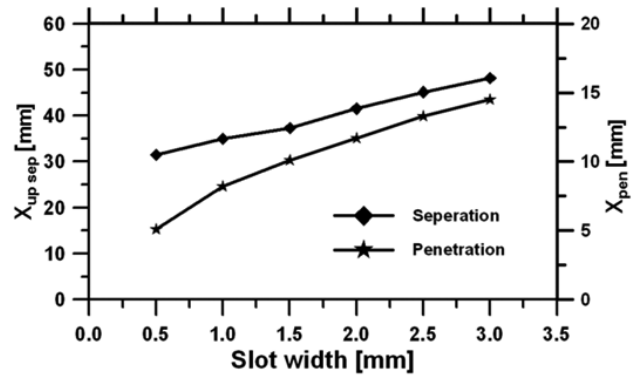


Figure 14. Maximum upstream separation distance and penetration height for different slot widths.

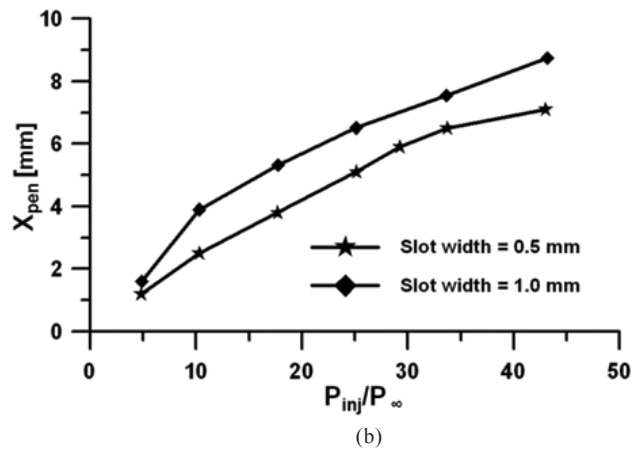
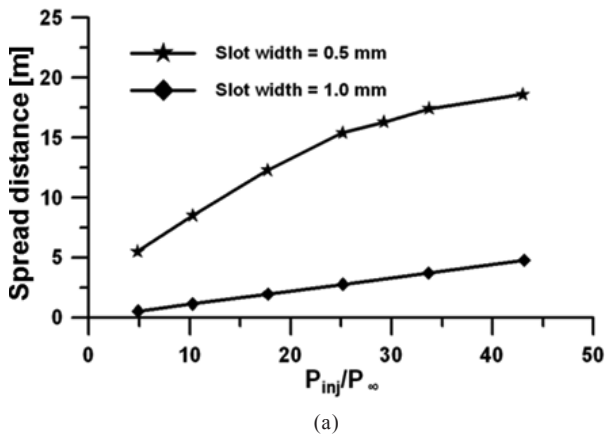


Figure 15. Maximum (a) spread and (b) penetration height for different free stream – to – jet pressure ratios.

5. CONCLUSIONS

Transverse sonic injection into a supersonic flow field is explored numerically with a 3D RANS solver and two equation turbulence models. Comparison of wall pressures with three different grids demonstrates the grid independence of the results. RNG- $k\epsilon$ turbulence model better predicts the experimental wall pressure upstream of the injection compared to the other three turbulence models ($k\epsilon$, $k\omega$, SST- $k\epsilon$). Whereas in the downstream of the injection, all the turbulence models provide almost identical results. Computed wall pressures compare well with experimental data for different slot injection pressures. With the increase in jet-to free stream pressure causes more penetration of the injectant in downstream region and cause more total pressure loss. The extent of upstream separation increases with slot injection pressure and computed separation lengths match well with test data. Increase in the slot width also enhances the interaction between free stream and secondary flow and causes more spreading and penetration of the injectant in the downstream.

REFERENCES

- Huang, W.; Pourkashanian, M.; Ma, L.; Ingham, D.B., Luo, S.B. & Wang, Z.G. Investigation on the flame holding mechanisms in supersonic flows: Backward facing step and cavity flameholder. *J. Visualization*, 2011, **14**(1) 63–74.
doi: 10.1007/S12650-010-0064-8
- Huang, W.; Luo, S.B.; Liu, J. & Wang, Z.G. Effect of cavity flame holder configuration on combustion flow field performance of integrated hypersonic vehicle. *Sci. China Technol. Sci.* 2010, **53**(10), 2725–2733.
doi: 10.1007/S11431-010-4062-9
- Brandeis, J. & Gill, J. Experimental investigation of side-jet steering for supersonic and hypersonic missiles. *J. Spacecraft Rockets*, 1996, **33**(3), 346–352.
doi: 10.2514/3.26766
- Min, B.Y.; Lee, J.W. & Byun, Y.H. Numerical investigation of the shock interaction effect on the lateral jet controlled missile. *Aerosp. Sci. Technol.*, 2006, **10**, 385–393.
doi: 10.1016/j.ast.2005.11.013
- Spaid, F.W. & Zukoski, E.E. A study of the interaction of gaseous jets from transverse slots with supersonic external flows. *AIAA Journal*, 1968, **6**(2), 205–212.
doi: 10.2514/3.4479
- Spaid, F.W. Two-dimensional jet interaction studies at large values of Reynolds and Mach numbers. *AIAA Journal*. 1975, **13**(11) 1430–1434.
doi: 10.2514/3.7011
- Portz, R. & Segal, C. Penetration of gaseous jets in supersonic flows. *AIAA Journal*. 2006, **44**(10), 2426–2429.
doi: 10.2514/1.23541
- Aso, S.; Okuyama, S.; Kawai, M. & Ando, Y. Experimental study on mixing phenomena in supersonic flows with slot injection. AIAA Paper No. 91-0016.
- Weinder, E.H. & Drummond, J.P. Numerical study of staged fuel injection for supersonic combustion. *AIAA Journal*, 1982, **20**(10), 1426-1431.
doi: 10.2514/3.51202
- Rizzeta, D.P. Numerical investigation of slot jet injection into a turbulent supersonic stream. AIAA Paper No. 92-0839.
- Clark, S.W. & Chan, S.C. Numerical investigation of a transverse jet for supersonic aerodynamic control. AIAA Paper No. 92-0639.
- Chenault, C.F. & Beran, P.S. K- ϵ and Reynolds stress turbulence model comparisons for two dimensional injection flows. *AIAA Journal*, 1998, **36**(8), 1401-1412.
doi: 10.2514/2.561
- Uenishi, K.; Rogers, R.C. & Northam, G.B. Numerical predictions of a rearward-facing-step flow in a supersonic combustor. *J. Propulsion Power*, 1989, **5**(2), 158-164.
doi: 10.2514/3.23131
- Segal, C.; Haj-Hariri, H. & McDaniel, J.C. A numerical investigation of hydrogen combustion in Mach 2 airflow. *AIAA Paper no.* 92-0341.
- Lee, S.H. & Mitani, T. Mixing augmentation of transverse injection in scramjet combustor. *J. Propulsion Power*, 2003, **19**(1), 115-124.
doi: 10.2514/2.6087
- Sriram, A.T. & Mathew, J. Numerical simulation of transverse injection of circular jets into turbulent supersonic streams. *J. Propulsion Power*, 2008, **24**(1), 45-54.
doi: 10.2514/1.26884
- Chenault, C.F.; Beran, P.S. & Bowersox, R.D.W. Numerical investigation of supersonic injection using a Reynolds stress turbulence model. *AIAA Journal*, 1999, **37**(10), 1257-1269.
doi: 10.2514/2.594
- Huang, W.; Liu, W.; Li, S.; Xia, Z.; Liu, J. & Wang, Z. Influence of turbulence model on the transverse slot injection flow field in supersonic flow. *Acta Astronautica*, 2012, **73**(1), 1-9.
doi: 10.1016/j.actaastro.2011.12.003
- Won, S.H.; Jeung, I.S.; Parent, B. & Choi, J.Y. Numerical investigation of transverse hydrogen jet into supersonic cross flow using detached eddy simulation. *AIAA Journal*, 2010, **48**(6), 1047-1058.
doi: 10.2514/1.41165
- Kawai, S. & Lele, S.K. Large eddy simulation of jet mixing in supersonic cross flows. *AIAA Journal*, 2010, **48**(9), 2063-2083.
doi: 10.2514/1.J050282
- Peterson, D.M. & Candler, G.V. Hybrid Reynolds averaged and large eddy simulation of normal injection into supersonic cross flow. *J. Propulsion Power*, 2010, **26**(3), 533-544.
doi: 10.2514/1.46810
- ANSYS CFX software, Release 14.5: Installation and Overview, January 7th, 2013.

CONTRIBUTORS

Mr Malsur Dharavath obtained his ME (Aerospace Engineering) from Indian Institute of Science (IISc), Bengaluru. He is working in the DRDO-Defence Research and Development Laboratory, Hyderabad. He has about 20 journal papers and 19 conference papers to his credit. His research areas includes: Scramjet and hypersonic propulsion system, combustion modelling, free and confined supersonic jets applicable to missile propulsion. Contribution in the current study, he has generated the grid, setup the problem, carried out numerical simulations and post processed the results.

Dr P. Manna obtained his PhD (Thermal Science and Engineering) from IIT, Kharagpur. Presently he is working as a Scientist in the Directorate of Computational Dynamics, DRDO-Defence Research and Development Laboratory, Hyderabad. He has published 25 journals papers and 28 conference papers. His research interests include: CFD, propulsion, heat transfer, and high-speed reacting flow. Contribution in the current study, he has carried out numerical simulation, analysed the results and contributed in the manuscript preparation

Dr Debasis Chakraborty obtained his PhD (Aerospace Engineering) from Indian Institute of Science (IISc), Bengaluru. Presently, he is working as Technology Director, Computational Dynamics, DRDO-Defence Research and Development Laboratory, Hyderabad. He has about 98 journal papers and 119 conference papers to his credit. His research areas includes: CFD, aerodynamics, high speed combustion and propulsion. Contribution in the current study, he has provided overall guidance in the simulation and data analysis. He prepared the final manuscript